Plant Molecular Biology (2024) 114:91
https://doi.org/10.1007/s11103-024-01488-z

OsIPK1 frameshift mutations disturb phosphorus homeostasis and impair starch synthesis during grain filling in rice

Lina Wang[1] · Jing Cui[1] · Ning Zhang[1] · Xueqin Wang[1] · Jingping Su[3] · María Pilar Vallés[4] · Shian Wu[1] · Wei Yao[1] · Xiwen Chen[2] · Defu Chen[1,5]

Received: 7 April 2024 / Accepted: 10 July 2024

Abstract

Inositol 1,3,4,5,6-pentakisphosphate 2-kinase (IPK1) catalyzes the final step in phytic acid ($InsP_6$) synthesis. In this study, the effects of *OsIPK1* mutations on $InsP_6$ synthesis, grain filling and their underlying mechanisms were investigated. Seven gRNAs were designed to disrupt the *OsIPK1* gene via CRISPR/CAS9 system. Only 4 of them generated 29 individual insertion or deletion T_0 plants, in which nine biallelic or heterozygous genotypes were identified. Segregation analysis revealed that *OsIPK1* frameshift mutants are homozygous lethality. The biallelic and heterozygous frameshift mutants exhibited significant reduction in yield-related traits, particularly in the seed-setting rate and yield per plant. Despite a notable decline in pollen viability, the male and female gametes had comparable transmission rates to their progenies in the mutants. A significant number of the filling-aborted (FA) grains was observed in mature grains of these heterozygous frameshift mutants. These grains exhibited a nearly complete blockage of $InsP_6$ synthesis, resulting in a pronounced increase in Pi content. In contrast, a slight decline in $InsP_6$ content was observed in the plump grains. During the filling stage, owing to the excessive accumulation of Pi, starch synthesis was significantly impaired, and the endosperm development-specific gene expression was nearly abolished. Consistently, the activity of whereas AGPase, a key enzyme in starch synthesis, was significantly decreased and Pi transporter gene expression was upregulated in the FA grains. Taken together, these results demonstrate that *OsIPK1* frameshift mutations result in excessive Pi accumulation, decreased starch synthesis, and ultimately leading to lower yields in rice.

Key message

OsIPK1 frameshift mutation results in excessive Pi accumulation in the filling-aborted grain and reduced grain yield in rice.

Keywords OsIPK1 · Phytic acid · Homozygous lethality · Starch synthesis · Rice

✉ Xiwen Chen
xiwenchen@nankai.edu.cn

✉ Defu Chen
chendefu@nankai.edu.cn

1 Department of Genetics and Cell Biology, College of Life Sciences, Nankai University, Tianjin 300071, China

2 Department of Biochemistry and Molecular Biology, College of Life Sciences, Nankai University, Tianjin 300071, China

3 Tianjin Key Laboratory of Crop Genetics and Breeding, Crop Research Institute, Tianjin Academy of Agricultural Sciences, Tianjin 300384, China

4 Department of Genetics and Plant Breeding, Aula Dei Experimental Station, Spanish National Research Council (EEAD-CSIC), Zaragoza 50059, Spain

5 Southwest United Graduate School, Kunming 650092, China

Introduction

Phytic acid, also known as *myo*-inositol-1,2,3,4,5,6-hexakisphosphate ($InsP_6$), is the primary storage form of phosphorus (P) in plant seeds (Freed et al. 2020), accounting for 65%-85% of total seed P content (Raboy 1997a). However, monogastric animals (including humans) cannot degrade $InsP_6$ owing to the lack of endogenous phytase. This means that the phosphorus present in the cereals is not available. The excretion of undigested $InsP_6$ through waste results in environmental P pollution, which accelerates eutrophication (Sharpley et al. 1994; Raboy 2000). In addition, $InsP_6$ is a strong chelator of nutritionally important divalent cations such as Ca^{2+}, Fe^{2+}, Mg^{2+}, Mn^{2+} and Zn^{2+} (Raboy 2001; Cominelli et al. 2020), thereby reducing their nutritional

Published online: 22 August 2024

value (Al Hasan et al. 2016). Based on these considerations, *low phytic acid* (*lpa*) breeding was first proposed in the 1990s (Raboy 2000), and the first *lpa* maize mutants were obtained in 1997 (Raboy 1997b). Subsequently, several studies have been conducted based on targeted mutations of genes involved in $InsP_6$ synthesis, resulting in the development of new *lpa* germplasm in crops such as wheat, rice, maize, barley, soybean, pea, and canola (reviewed by Wang et al. 2022; Sahu et al. 2024).

$InsP_6$ can be synthesized by two interconnected pathways in plants: lipid-dependent and -independent pathways. In the lipid-dependent pathway, phospholipase C hydrolyzes phosphatidylinositol phosphate to form $Ins(1,4,5)P_3$, which is then sequentially phosphorylated to $InsP_4$ and $InsP_5$ by a dual-specific inositol polyphosphate kinase (IPK2) (Saiardi et al. 1999; Stevenson-Paulik et al. 2002, 2005). In the lipid-independent pathway, inositol-3-phosphate synthase (MIPS) catalyzes the conversion of glucose-6-phosphate to inositol-3-phosphate ($InsP_1$) (Shi et al. 2005; Kim and Tai 2011), which is then sequentially phosphorylated to form inositol-1,4,5-triphosphate $Ins(1,4,5)P_3$, $Ins(1,4,5,6)P_4$ and $Ins(1,3,4,5,6)P_5$ by inositol-1,3,4-trisphosphate-5/6-kinases (ITPKs) (Wilson and Majerus 1997; Yang and Shears 2000). Both pathways utilize inositol 1,3,4,5,6-pentakisphosphate 2-kinase (IPK1) to catalyze the conversion of $Ins(1,3,4,5,6)P_5$ to $InsP_6$ (Verbsky et al. 2002; Cridland and Gillaspy 2020), suggesting the importance of IPK1 in $InsP_6$ synthesis. The gene encoding IPK1 has been selected as a target for *lpa* wheat germplasm development using RNAi (Aggarwal et al. 2018) or CRISPR/Cas9 technology (Ibrahim et al. 2022), in which the $InsP_6$ content in grains decreased and the availability of phosphorus, iron, and zinc increased.

Comparison of the phenotypes after mutating *IPK1* in different plant species indicated that mutants exhibited decreased $InsP_6$ content, however displayed different or contradictory agronomic traits. For example, *Arabidopsis IPK1* T-DNA insertion mutants reduced the $InsP_6$ content by 83%, however did not alter other traits (Stevenson-Paulik et al. 2005), which was also the case for a soybean mutant with the *IPK1* gene mutated at $G_{1520}>A$ (Yuan et al. 2012). *IPK1* rice transgenic lines (Ali et al. 2013) and wheat mutants (Ibrahim et al. 2022), which were developed by RNAi or CRISPR/Cas9, also exhibited little change in agronomic traits, such as seed setting rate and yield. In contrast, the loss-of-function *Arabidopsis IPK1* mutant (null mutant) *atipk1-2/3* exhibited severe growth retardation and was unable to complete its life cycle, whereas *atipk1-1* exhibited enhanced inorganic phosphorus (Pi) uptake through the roots, and increased root crown Pi transfer capacity (Kuo et al. 2014). Moreover, in some T-DNA insertion mutants, the root system displayed significant Pi starvation, hypersensitivity to arsenic (Sun et al. 2016), and susceptibility to the plant pathogen *Pseudomonas syringae* (Poon et al. 2020). Recently, *OsIPK1* was knocked out using CRISPR/Cas9 technology, and only a homozygous rice mutant with a 33-base deletion in the third exon was obtained (Jiang et al. 2021). The mutant displayed a 19.5% reduction in $InsP_6$ content and enhanced salt and drought tolerance. No change in its agronomic traits was observed. However, homozygous frameshift mutants could not be obtained, and were not further investigated (Jiang et al. 2021). Therefore, whether lowering $InsP_6$ levels by mutating *IPK1* affects agronomic traits remains unclear.

In cereal crops such as rice, grain filling is a crucial process in which fertilized ovaries acquire the carbohydrates produced by leaves to synthesize starch. As starch accounts for more than 70% of the dry weight of rice seeds, changes in starch biosynthesis greatly influences the yield of cereals. ADP-glucose pyrophosphorylase (AGPase) catalyzes glucose-1-P and ATP and produces ADP-glucose (ADPG), an activated glucosyl donor for starch synthesis (Pfister and Zeeman 2016). AGPases are heterotetramers composed of two large subunits (AGPL) and two small subunits (AGPS) (Huang et al. 2014). Both AGPL and AGPS are localized in the cytosol and plastids, and the cytosolic type accounts for most AGPase activity in the cereal endosperm (Jeon et al. 2010; Saripalli and Gupta 2015). In contrast, glucose-6-P participates in the synthesis of $InsP_6$. Disruption of the enzymes involved in $InsP_6$ synthesis resulted in a several-fold increase in seed Pi (Liu et al. 2007; Yuan et al. 2007; Ali et al. 2013; Li et al. 2014; Aggarwal et al. 2018). Therefore, the maintenance of normal cytoplasmic Pi levels (P homeostasis) is crucial for seed development, as AGPase, a key enzyme in starch synthesis, is allosterically inhibited by Pi (Preiss 1982). However, the mechanisms underlying phosphate homeostasis in starch biosynthesis and grain yield in cereals are poorly understood.

Rice is an important global food crop (Fitzgerald et al. 2009), and its $InsP_6$ content ranks among the top 134 common plant species (Silva et al. 2021), so it is of great significance to cultivate *lpa* rice. The rice genome contains only one copy of *OsIPK1* (*Os04g56580*) (Suzuki et al. 2007), which is located on chromosome 4. Whether using it as a target for rice *lpa* breeding lacks systematic evaluation. Previously, the *g2* and *g4* sites of *OsIPK1* were edited using CRISPR/Cas9, and only one mutant with a 3-base deletion at the *g4* site was obtained (Li et al. 2019). In this study, seven gRNAs distributed across the whole *OsIPK1* were designed, and only four gRNAs produced base insertions and deletions (indels). Segregation analysis revealed that *OsIPK1* frameshift mutants are homozygous lethality. A quarter of grains in the heterozygous frameshift mutants exhibited excessive Pi accumulation, diminished AGPase activity, and blocked conversion of sucrose into starch. Our results provide insights into the manipulation of $InsP_6$ synthesis and *lpa* breeding in rice and other cereal crops.

Materials and methods

Plant materials and growth conditions

Rice cultivar variety JinGeng 818 (*Oryza sativa* L. ssp. *Japonica*, national authorized variety 2014046, WT) was used for this study. The derived *OsIPK1-indel* mutants were grown in a controlled glasshouse or paddy field with routine management practices: single-plant planting, single-plant harvesting, and single-plant testing. Materials grown in a controlled glasshouse were used for evaluating genotypes, physicochemical parameters, and gene expression, while those grown in paddy fields were used for propagation, agronomic trait evaluation, and artificially assisted reciprocal crosses. The three ecological sites were Tianjin (39° 06′ 06″ N/117° 10′ 03″ E, T_0, in spring 2019; T_5, in spring 2022), Hainan (18° 20′ 17″ N/109° 38′ 55″ E, T_1, in winter 2019; T_3, in winter 2020 and T_4, in winter 2021) and Anhui (32° 40′ 09″ N/118° 37′ 22″ E, T_2, in spring 2020).

gRNA design, CRISPR/Cas9 vector construction, and generation of *OsIPK1-indel* mutants and their complementation lines

The gRNAs were designed using the CRISPR-P 1.0 (http://crispr.hzau.edu.cn/CRISPR/). The single-stranded DNA of each target sequence (Table S1) was synthesized and complemented to form oligomers. CRISPR/Cas9 vectors containing distinct gRNA sequences were constructed by inserting oligomers into the *Bsp*QI site of the binary vector VK005-01 (Viewsolid Biotech. Co., Beijing, China), the derived vectors were named VK with serial numbers, and mature embryo-derived calli were transformed using *Agrobacterium tumefaciens* strain EHA105 as described by Li et al. (2019). To obtain complementation lines, the promoter of *OsIPK1* (2.2 kb DNA fragment, abbreviated as *ProOsIPK1-2.2 kb*) was cloned by PCR using the primer pair IPK1-Pro-F/IPK1-Pro-R (Table S2) and then inserted into the *Nco*I/*Bst*EII-digested pCAMBIA1301 vector to replace the *CaMV35S* promoter and drive the expression of the cDNA of *OsIPK1* amplified using the primer pair IPK1-cDNA-F/IPK1-cDNA-R (Table S2). The resulting constructs were transformed into mature embryo-derived calli using the same method.

Genotyping and genetic analysis of *OsIPK1-indel* mutants

To analyze the genotype of the transgenic plants in each gRNA site, genomic DNA was extracted from leaves of transgenic T_0 lines by using the CTAB method (Doyle 1991). The genomic region of each gRNA site was amplified using specific primers (Table S2) and then genotyped by Sanger sequencing. The TA cloning was performed if the sequencing peak overlapped, and 10 colonies were sequenced to determine their genotypes. Genotyping of the progenies was also performed using a similar method and the segregation frequency was calculated.

The transgene-free *OsIPK1-indel* plants were identified by amplifying the leaf DNA of the T_1 generation using the primers hpt-F/hpt-R (for *hygromycin* gene), VK005-1-F/VK005-1-R (for *rU6*-gRNA) and Cas-sun-F/Cas-sun-R (for *mpCas9*) (Table S2). Off-target analysis was conducted using the PCR-sequencing method (primers are shown in Table S3). Transgene-free lines with non-off-target effects were used for propagation analysis.

Agronomic trait analysis and artificial-assisted reciprocal cross

OsIPK1-indel mutant seedlings (at least 40 plants for each genotype) were planted in an experimental paddy field under natural conditions. Plant height, effective tiller number, grain number per panicle, grain setting rate, 1000-grain weight, and yield per plant were measured for 15 plants of each genotype at random, on a single-plant basis, at the mature stage. To eliminate the generational and ecological environment influences, the values of each trait were converted into relative values of the WT in the corresponding year.

Artificially assisted reciprocal crosses were performed in fields between WT and *OsIPK1-indel* mutants with the same flowering time. After cutting out the immature florets or those that were pollinated in the female parent panicles, 50–80 pre-flowering mature florets remained for emasculation. At noon, the paternal pollens were pollinated to the emasculated female parent florets. Hybrid seeds were collected after 25 days, and germinated and genotyped as described above.

$InsP_6$, Pi, total Pi, and carbohydrate analysis

The hulled grains were ground into powder using a tissue grinder (Shanghai Jingxin Industrial Development Co. Ltd., Shanghai, China). For $InsP_6$ analysis, 1 g of powder was taken and analyzed using a K-PHYT kit (Megazyme International, Wicklow, Ireland), following the instructions provided by the suppliers. This method involved the acid extraction of inositol phosphates, followed by treatment with phytase and alkaline phosphatase. The total phosphate released was measured using a modified colorimetric method, and $InsP_6$ content was calculated. For Pi content analysis, 0.15 g of powder was mixed with 15 mL of 12.5% (*w/v*) trichloroacetic acid solution (with 25 mM $MgCl_2$), extracted overnight at 4 °C, and then centrifuged at

15,000×*g* at 4 °C for 15 min. The supernatant was filtered through a 0.22 μm filter, adjusted to pH 3 with 0.5 M sulfuric acid, and diluted to 25 mL to obtain the Pi extract. The Pi content was determined using molybdenum-antimony scandium colorimetry (Murphy and Riley 1962), and the A_{700} value was determined. For total phosphorus content analysis, 0.5 g powder was mixed with 10 mL HNO_4-HCl (9:1, *v/v*) and kept in an acid catcher at 120 °C for 1 h. After filtration with a 0.22 μm filter, the extracted solution (0.5 mL) was diluted to 25 mL, and the total phosphorus was extracted. The Pi content was determined as described above, and the total phosphorus in the sample was calculated.

Starch, soluble sugar, and sucrose contents were determined using an Amylum Content Assay Kit, Plant Soluble Sugar Content Assay Kit, and Plant Sucrose Content Assay Kit (all provided by Sangon Biotech (Shanghai) Co., Ltd., Shanghai, China), respectively, according to the manufacturer's instructions. The starch and soluble sugar contents were determined by the anthrone colorimetric method; the sucrose content was determined by detecting the colored substance produced by the reaction of sucrose hydrolysate fructose with resorcinol at 480 nm.

Pollen viability examination

To observe the characteristics of pollen grains, pollen grains were shed onto a glass slide, and then 2% (*w/v*) iodine-potassium-iodide (I_2-KI) solution was added. After 5 min, their morphological characteristics were observed under light microscope (S9i, Leica) and counted fully stained, partially stained, and not stained pollen, separately.

Observation of mature or developing grains

Mature grains were carefully broken apart with forceps, and cut with a cutter, and the cross-sections of the grains were subsequently stained with 2% (*w/v*) I_2-KI solution. For the developing grains, those in the middle and upper panicles (15 days after flowering) were selected, incised with a razor blade, squeezed with tweezers, and subsequently observed and photographed under a microscope (S9i, Leica). To observe the longitudinal sections of the grains, dehulled grains at the filling stage were collected, embedded, sectioned as described previously (Wang et al. 2015), stained with 0.1% toluidine blue, and observed under a light microscope (S9i, Leica).

Gene expression analysis and AGPase activity determination

The hulled grains were collected during the filling stage, and total RNA was extracted using the Eastep™ Super Total RNA Extraction Kit (Promega, Madison, WI, USA). First-strand cDNAs were synthesized using Reverse Transcriptase M-MLV (RNase H⁻) [TaKaRa Biotechnology (Dalian) Co., Ltd, Dalian, China], and qRT-PCR was performed using TB Green® Premix Ex Taq™ II (Tli RNaseH Plus) (TaKaRa) on a quantitative fluorescence PCR instrument CFX96 (Bio-Rad, Hercules, CA, USA). *OsPYL3-like* (*Os06g0528300*), *OsAGPL2* (*Os01g0633100*), and *OsAGPS2b* (*Os08g25734*) were selected as endosperm-specific genes. Four upstream genes [*OsMIPS* (*Os03g09250*), *OsIMP* (*Os03g0587000*), *OsITPK1* (*Os10g01480*) and *OsIPK1* (*Os04g56580*)], two downstream genes [*OsVIP1* (*Os01g0777700*) and *OsVIP2* (*Os03g0689100*)] involved in $InsP_6$ synthesis, and two phosphorus transport genes, *OsPHO1;2* (*Os02g56510*) and *OsPHT1;3* (*Os10g30770*), were used for gene expression analysis. The *actin* gene (*Os03g50885*) was used as an internal control. qRT-PCR primers are shown in Table S2.

Developing grains were dehulled and ground into powder in liquid nitrogen. AGPase activity was determined as described by Ma et al. (2021).

Statistical analysis

To analyze the significant differences among multiple groups, one-way analysis of variance (ANOVA) followed by Tukey's test at $p < 0.05$ was adopted. Statistical significance between two groups was assessed by two-tailed Student's *t*-test. All statistical tests were performed using IBM SPSS Statistics 22.0 software.

Results

OsIPK1 frameshift mutations are homozygous lethality

Seven guide RNAs (gRNAs) (*g1–g7*) distributed throughout the *OsIPK1* gene (Fig. 1) were designed, and their CRISPR/Cas9 vectors were constructed and transformed into mature embryo-derived calli, respectively. A total of 151 transgenic plants were regenerated from 5689 transformed calli. Of them, only 29 plants from four gRNAs (*g1*, *g3*, *g4*, and *g7*) resulted in indels (base insertions or deletions) (Fig. S1A), with a 19.2% indel frequency. The indel frequencies were the highest for *g1* (73%), followed by *g7* (58%), *g4* (14%), and *g3* (3%), with no indels observed for the other gRNAs (Fig. S1B). To obtain detailed genotypic information, the target fragments were subjected to TA cloning and sequencing. Nine biallelic and heterozygous mutants were identified, including five (*−8+5/+1*, *−3/+1*, *−3/−16*, *−3/−25*, and *−15/+1*) from *g1*, two (*0/+1* and *0/−1*) ("*0*" indicates no mutation, similarly hereinafter) from *g7*, and only one from *g3* (*0/−4*) and *g4* (*0/+1*), respectively (Table 1).

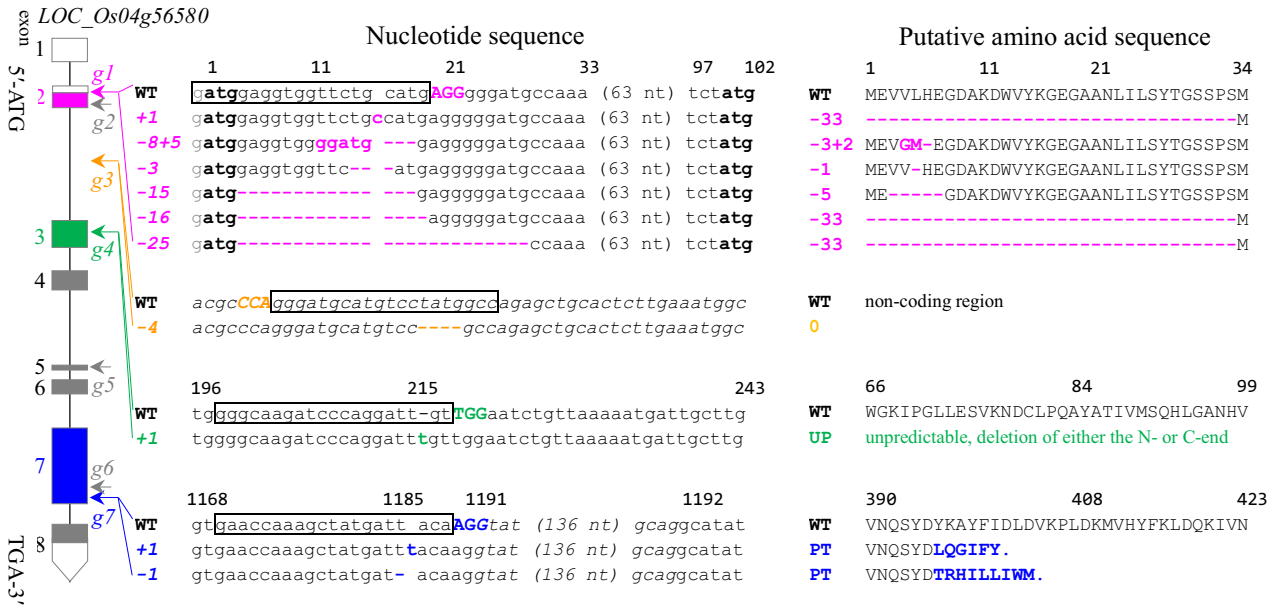

Fig. 1 Distribution of seven gRNAs across *OsIPK1* and its edited sequence analysis in *OsIPK1-indel* mutants. Left is a schematic diagram of *OsIPK1* (*Os04g56580*) and the localization of gRNAs. Different gRNAs are shown in different colors. The number above the sequence indicates the position of the coding sequence (CDS) and its deduced amino acid sequence in the wild type. The italic number with "+" or "−" in front of "nucleotide sequence" (e.g., *−8+5*) is the genotype of the mutant. The "Nucleotide sequence" behind the genotype is the *OsIPK1* mutant sequence. The normal letters are in the exon sequence, while the italic letters are in the intron sequence. The sequence with the box is the gRNA site, and the capital letter next to it is the protospacer adjacent motif (PAM) sequence. The indel sequence is shown in color, where the letter is the base insertion, while "-" is the base deletion. Their putative amino acid sequence deduced by Lasergene Software Suite ver 7.1 (DNASTAR Inc., Wisconsin, USA) is shown on the right, and the labeling method is roughly the same as before, except that capital letters are used. UP: unpredictable, PT: premature translation termination

Table 1 Genetic segregation analysis in progenies of the biallelic or heterozygous *OsIPK1-indel* mutants

Line	Parental genotype	Segregation pattern[a]			χ^2 value
g1	*−8+5/+1*	*−8+5/−8+5* (36)	*−8+5/+1* (63)	*+1/+1* (0)	0.41 for 1:2:0
	−3/+1	*−3/−3* (41)	*−3/+1* (57)	*+1/+1* (0)	3.19 for 1:2:0
	−3/−16	*−3/−3* (23)	*−3/−16* (37)	*−16/−16* (0)	0.68 for 1:2:0
	−3/−25	*−3/−3* (22)	*−3/−25* (34)	*−25/−25* (0)	0.89 for 1:2:0
	−15/+1	*−15/−15* (11)	*−15/+1* (31)	*+1/+1* (0)	0.96 for 1:2:0
g3	*0/−4*	*0/0* (8)	*0/−4* (11)	*−4/−4* (7)	0.69 for 1:2:1
g4	*0/+1*	*0/0* (11)	*0/+1* (17)	*+1/+1* (0)	0.45 for 1:2:0
g7	*0/+1*	*0/0* (90)	*0/+1* (214)	*+1/+1* (0)	1.90 for 1:2:0
	0/−1	*0/0* (18)	*0/−1* (21)	*−1/−1* (0)	2.88 for 1:2:0

The χ^2 analysis indicates that the segregation frequency is statistically significant

[a]Numbers in parentheses indicate the number of progenies with the genotype, which is the cumulative data for three successive generations (T_1, T_2, and T_3)

To obtain homozygous *OsIPK1-indel* lines, nine lines without transgenes or off-target genes were selected for self-crossing. Genotype identification for three consecutive generations (T_1, T_2, and T_3) revealed that homozygous in-frame mutants (*−8+5*, *−3*, and *−15*) could be obtained from *g1*, which caused deletions of several amino acids in the N-terminus of the protein. Homozygous in-frame mutants *−4* could be also obtained from *g3*, which was in the intron and would not affect the coding sequence. Unexpectedly, no homozygous frameshift mutants were identified. These frameshift mutations were the*+1*, *−16*, and *−25* from *g1* (which may lose 33 amino acid residues at the N-terminus), at*+1* from *g4* (which may lose either 71 amino acid residues at the N-terminus or 374 amino acid residues at the C-terminus), and at*+1* or *−1* from *g7* (which may lose 50 amino acid residues at the C-terminus sequence owing to a premature

termination). All these frameshift mutants exhibited a 1:2:0 progeny segregation frequency, implying that the frameshift mutants are homozygous lethal, but can exist normally as a recessive gene in biallelic or heterozygous plants (Table 1).

To further confirm that the homozygous lethality is caused by frameshift mutations of *OsIPK1*, the full-length coding sequence of *OsIPK1* driven by its native promoter (Fig. S2A) was introduced into mature seed-derived calli from *−3/−25(g1)* mutants. Sequence of the T_1 complementation lines showed a clear nonoverlapping map with a deletion of −25 bp (Fig. S2B). Segregation analysis of the progeny revealed a segregation pattern of a 4:8:3 (homozygous *−3/−3* plants, 13 biallelic *−3/−25*, and 2 homozygous *−25/−25*, respectively) ($\chi^2 = 1.66$), suggesting that homozygous frameshift mutants could be generated in the complementation lines. These results indicated that *OsIPK1* frameshift mutations are responsible for the homozygous lethality.

Biallelic and heterozygous frameshift mutants exhibit significantly reduced yield-related traits, especially seed-setting rate, and yield per plant

To investigate the role of *OsIPK1* in rice growth and development, six agronomic traits (plant height, number of effective tillers, grains per panicle, seed-setting rate, 1000-grain weight, and yield per plant) of three homozygous and nine biallelic and heterozygous mutants without off-target (Table S3) were observed for three generations (T_1, T_2, and T_3) in three experimental plots. Except for individual lines (such as *−8+5(g1)*) and individual trait (grains per panicle), most of them have been significantly decreased, especially seed setting rate and yield per plant (Figs. 2, S3A).

Interestingly, the *−8+5* mutants derived from *g1,* whether homozygous (*−8+5/−8+5(g1)*) or biallelic (*−8+5/+1(g1)*) exhibited better plant height, number of effective tillers, grains per panicle, and yield per plant, compared to the wild-type (WT), with homozygotes being the most significant. For example, the average plant height and yield per plant of homozygotes in the three generations were 118.7 and 139.3%, respectively, and those of biallelic mutants were 114.1 and 114.0%, respectively, of the WT (Figs. 2, S3B). However, the *−3/−3(g1)* mutants that which had the same base deletions as *−8+5/−8+5(g1)*, displayed no significant differences in their agronomic traits with respect to WT (Figs. 2, S3C).

In contrast, all biallelic and heterozygous frameshift mutants exhibited significantly reduced seed-setting rates and reduced yields per plant (Fig. 2). The seed-setting rate ranged from 52.2% in *0/+1(g4)* to 83.2% in *−3/−25(g1)* of the wild-type (WT). The yield per plant ranged from 48.6% in *0/+1(g4)* to 76.5% of the WT in *−3/−16(g1)*. The *−4/−4(g3)* displayed no difference in the six agronomic traits compared to the WT owing to the intron position of *g3*. Taken together, these results indicated that *OsIPK1* frameshift mutations decreased seed-setting rates and yields per plant in rice.

Biallelic and heterozygous frameshift mutants exhibit lower pollen viability, however are not responsible for homozygous lethality

The fertility of frameshift mutants was examined as possible cause of their lethality. Mature florets in these lines did not show any noticeable morphological abnormalities (Fig. 3A). I_2-KI staining revealed three types of pollens: fully stained, partially stained, and not stained (Fig. 3B). Homozygous in-frame mutants (*−8+5/−8+5(g1)*) had similar proportions of the three pollen types to those of the WT. In contrast, biallelic and heterozygous frameshift mutants (except *−8+5/+1(g1)*) exhibited significantly lower proportions of fully stained pollen, which was only 58.9% of the WT (Fig. 3C). As these frameshift mutants produced two types of pollens, one with frameshift mutation and the other with in-frame mutation, we thus speculate only pollens with frameshift mutation, but not in-frame mutation, decreased their viability.

To further investigate whether lowered pollen viability is responsible for homozygous lethality in biallelic and heterozygous frameshift mutants, reciprocal crosses were performed between WT and five mutants whose flowering times were similar to those of the WT. All reciprocal crosses showed a 1:1 progeny segregation frequency (Table 2). The fertility of both the male and female gametes in the frameshift mutants suggests that homozygous lethality in these mutants may relate to zygotic development.

The filling-aborted (FA) grains are responsible for the reduced seed-setting rate in the *OsIPK1* frameshift mutants

To further investigate why homozygous lethality in frameshift mutants, the mature grains were observed after self-fertilization. Except for the plump grains, two types of unfilled grains were observed (Fig. 4A). One was a wizened grain with a normal seed coat, no starchy endosperm, and that could not be stained with the I_2-KI solution. As the grain might have been fertilized but failed to fill, it was named as a filling-aborted (FA) grain. The other was an unfertilized empty grain with a visible stigma and an undeveloped ovary, which also could not be stained with the I_2-KI solution. This grain was named as an empty grain.

Among the 11 genotypes studied (excluding *−4/−4(g3)* which had similar agronomic traits as WT, and *0/−1(g7)* which had the same agronomic traits as *0/+1(g7)*, respectively), WT had the lowest FA (0.64%) and empty grain

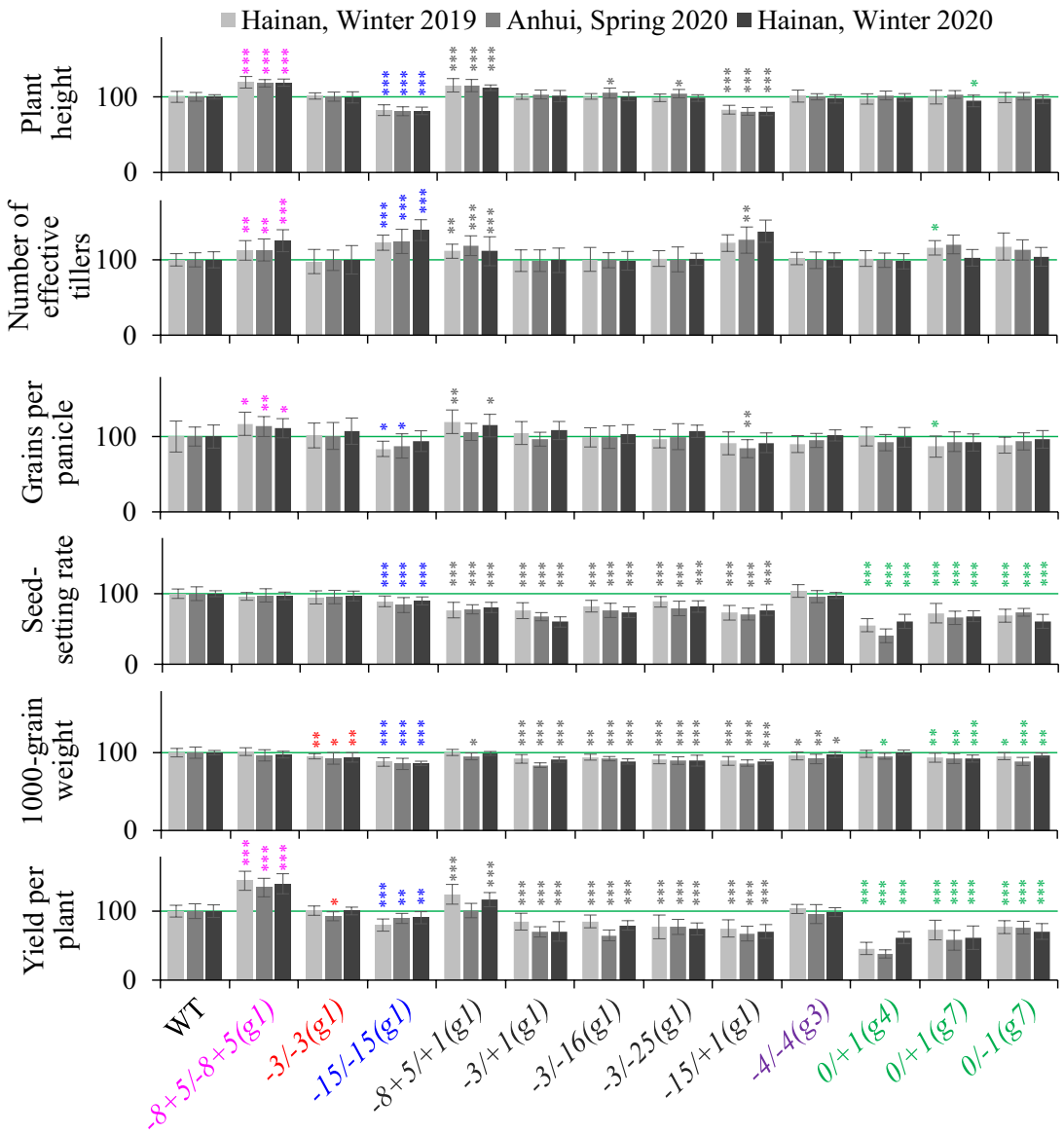

Fig. 2 Six agronomic traits in *OsIPK1-indel* mutants. The Y-axis is the relative ratio of agronomic traits in the *OsIPK1-indel* mutants compared to the corresponding WT under the same generation and ecological conditions. Data are shown as means ± SE (%) ($n = 15$ plants) (Student's *t*-tests: *, $P < 0.05$; **, $P < 0.01$; ***, $P < 0.001$, no difference if there is no asterisk)

(16.03%) rates, whereas *0/+1(g4)* had the highest FA (21.92%) and empty grain (28.66%) rates (Table S4).

Linear fit analysis revealed a negative correlation between the FA grain rate, empty grain rate, and the plump grain rate in these mutants, with the FA grain rate having a higher slope and a higher correlation coefficient ($k = -1.4151$ and $R^2 = 0.9534$) than the empty grain rate ($k = -2.5369$ and $R^2 = 0.8276$) (Fig. 4B). Moreover, the FA grain rate was almost zero in the WT, but was significantly higher in these biallelic or heterozygous mutants, that in *0/+1(g4)* (21.92%) nearly reached the theoretical Mendelian genetic segregation ratio (25% in recessive homozygote theory). Therefore, we proposed that FA grains were likely the abnormal zygote development after fertilization of frameshift male and female gametes, and were responsible for the reduced seed-setting rate in the *OsIPK1* frameshift mutants.

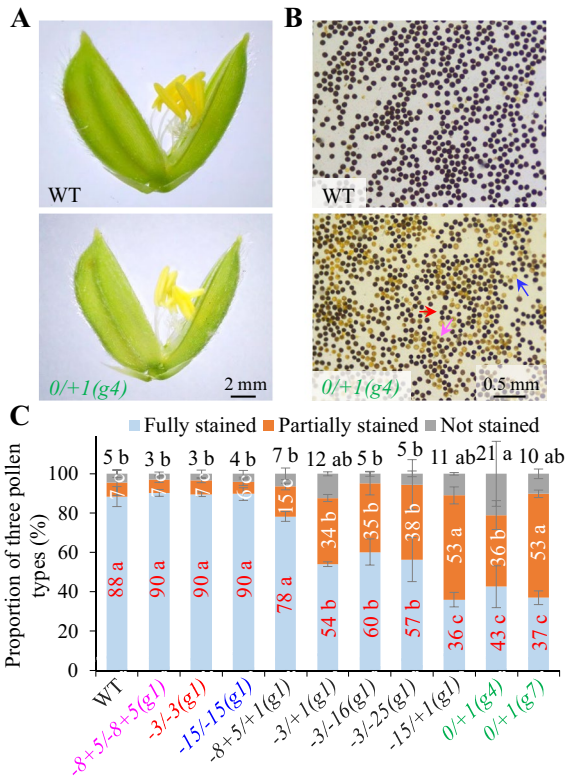

Fig. 3 Floret morphology and pollen viability in *OsIPK1-indel* mutants. **A** Floret morphology. **B** Pollen viability revealed by the I_2-KI staining method. Mature pollens with anther lengths exceeding 2/3 of florets were used for staining. Red, purple, and blue arrows represent fully stained, partially stained, and not stained pollen, respectively. **C** The proportion of three types of pollen in the *OsIPK1-indel* mutants. Data are shown as means ± SE (%) ($N = 3$ biological replicates; $n = 5$ spikelet). Different lowercase letters over bars indicate significant differences among the same type of pollen at $P < 0.05$ by one-way ANOVA

FA grains have a notably increased Pi content and decreased starch content

To investigate the effect of *OsIPK1* mutations on FA formation, $InsP_6$, inorganic phosphorus, and total phosphorus contents in the plump and FA grains of *OsIPK1-indel* mutants were determined. As *0/+1(g4)* and *0/+1(g7)* had a higher FA grain ratio, they were selected as the representative FA grains for testing.

All the *OsIPK1-indel* mutant plump grains had lower $InsP_6$ content (88.0–94.5%) but higher Pi content (101.6–211.1%) of the WT, except that *−8+5/−8+5(g1)* and *−8+5/+1(g1)* had slightly higher $InsP_6$ content (101.1–105.1%) and lower Pi content (67.0–73.9%) (Fig. 5). However, *0/+1(g4)* and *0/+1(g7)* had significantly lower $InsP_6$ content (44.5–57.6%) but much higher Pi content (41.8–43.5-fold) of the WT. No difference in total phosphorus content was detected between plump and FA grains of the mutants. These results indicated that *OsIPK1-indel* mutations result in an increased Pi content in plump grains, whereas a notably increased Pi content in FA grains, accompanied by a moderate decrease in $InsP_6$ content.

The starch, sucrose, and soluble sugar contents in the plump and FA grains of the *OsIPK1-indel* lines were determined. The plump grains of the *OsIPK1-indel* mutants (except *−8+5/−8+5(g1)* and *−8+5/+1(g1)*) had a slightly lower starch content (90.4–99.5%) and higher sucrose content (100.2–149.9%) of the WT. In contrast, a significant lower starch content (24.2–26.6%) and high sucrose content (3.61–3.83-fold) of the WT were detected in *FA(g4)* and *FA(g7)* grains (Fig. 5). However, the soluble sugar content displayed no regular pattern in the plump or FA grains of these *OsIPK1-indel* lines. In addition, a negative or positive correlation was observed between the Pi content and starch or sucrose content, respectively, in the plump seeds (Fig. S4). Taken together, these results suggested that as Pi levels in the grains increased, sucrose accumulated and starch decreased, probably due to an inhibition of the conversion of sucrose into starch.

$InsP_6$ in cereal crops is predominantly localized in the aleurone layer (clinging to bran) (Bohn et al. 2008). To investigate the distribution of $InsP_6$ and Pi in different tissues of the *0/+1(g4)*, *0/+1(g7)* lines and WT, levels were determined in the bran, embryos, and starchy endosperms of plump grains. $InsP_6$ and Pi predominantly occur in brans and embryos, few occur in the starchy endosperm, while their

Table 2 Segregation analysis of reciprocal crosses between biallelic or heterozygous *OsIPK1-indel* mutants and WT

Line	♀*OsIPK1-indel*×♂WT			♀WT×♂*OsIPK1-indel*		
	Segregation pattern[a]		χ^2 for 1:1	Segregation pattern[a]		χ^2 for 1:1
−3/−25(g1)	*0/−25* (43)	*0/−3* (55)	1.47	*0/−25* (48)	*0/−3* (54)	0.35
−3/−16(g1)	*0/−16* (27)	*0/−3* (37)	1.56	*0/−16* (40)	*0/−3* (44)	0.19
−3/+1(g1)	*0/+1* (32)	*0/−3* (35)	0.13	*0/+1* (25)	*0/−3* (36)	1.98
0/+1(g4)	*0/0* (44)	*0/+1* (31)	2.25	*0/0* (36)	*0/+1* (53)	3.25
0/+1(g7)	*0/0* (57)	*0/+1* (46)	1.17	*0/0* (51)	*0/+1* (63)	1.26

The χ^2 analysis shows that the segregation ratio in the table is statistically significant

[a]The numbers in parentheses indicate the number of progenies with this genotype

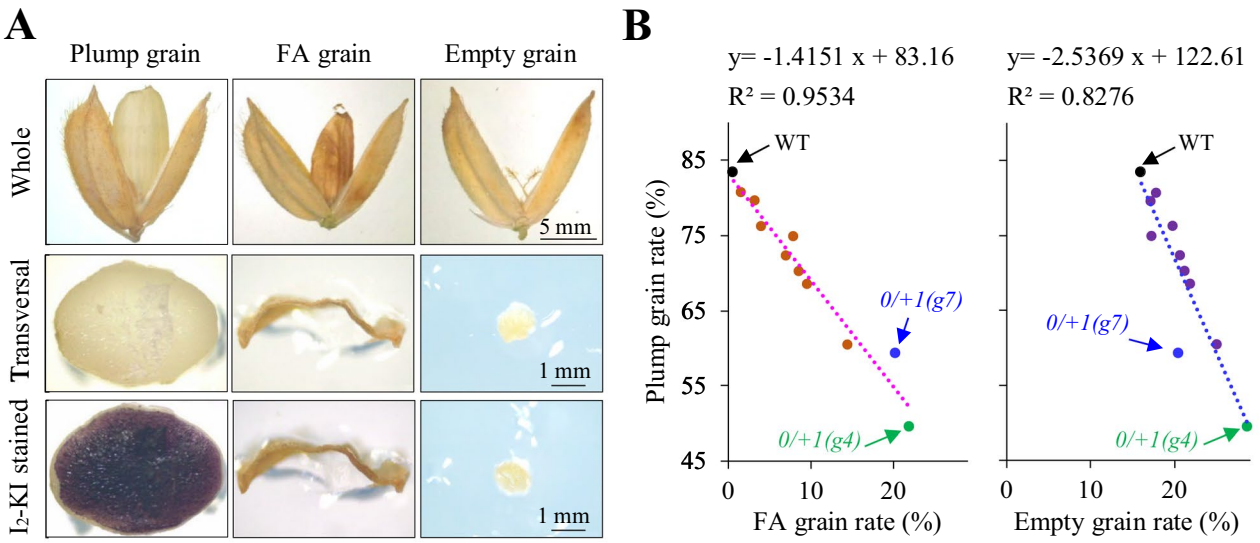

Fig. 4 Morphology of three types of mature grains and their linear correlation with the seed-setting rate in *OsIPK1-indel* mutants. **A** Comparison of whole grain, the cross-section of the dehulled grains, and their I_2-KI staining in mature plump grain, filling-aborted (FA) grain, and empty grain. **B** Correlation analysis between FA grain rate or empty grain rate with plump grain rate in *OsIPK1-indel* mutants. Dots are the mean values of *OsIPK1-indel* mutants. See Table S4 for detailed values

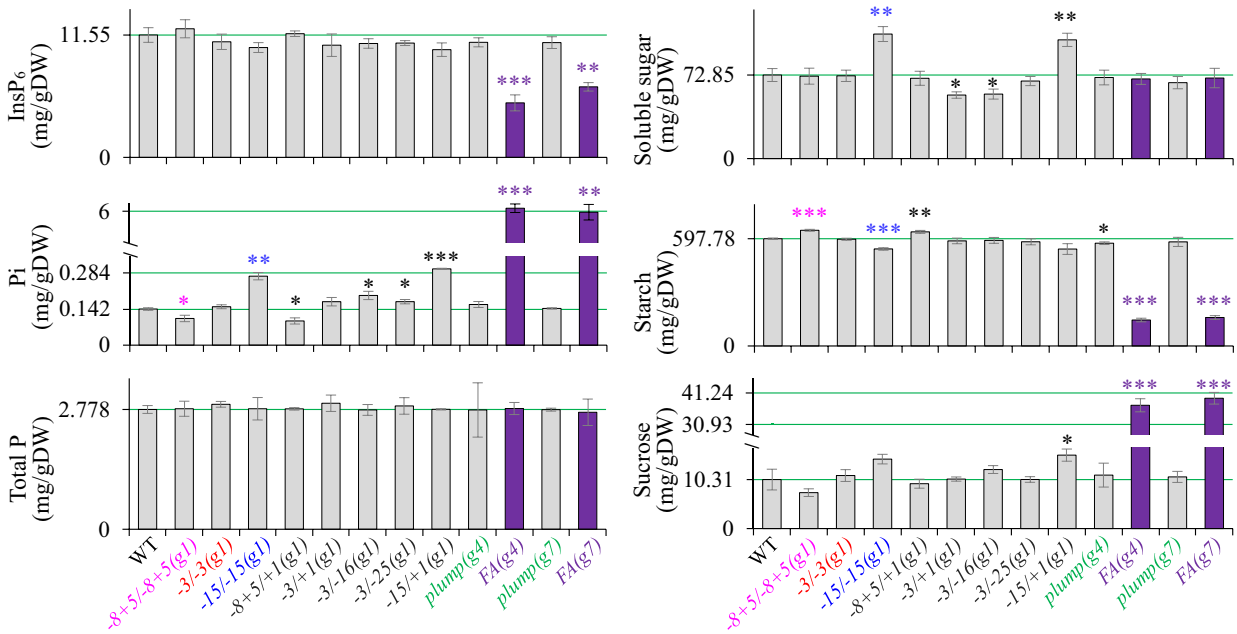

Fig. 5 $InsP_6$, inorganic phosphorus (Pi), total phosphorus (Total P), starch, soluble sugar, and sucrose contents in *OsIPK1-indel* mature grains. A horizontal line was drawn at the WT value. The portion above or below indicates an increase or decrease. Data are shown as means ± SE (mg/g DW) ($N = 3$ biological replicates; $n = 20$ grains) (Student's *t*-tests: *, $P < 0.05$; **, $P < 0.01$; ***, $P < 0.001$, no difference if there is no asterisk)

content in the bran of *FA(g4)* and *FA(g7)* was 5.2–7.3% and 5.4–6.4 folds of the bran of WT and plump grains, respectively (Fig. S5). Taken together, the frameshift mutants result in nearly complete blockage of $InsP_6$ synthesis in *FA(g4)* and *FA(g7)* grains, and excessive Pi accumulation, further suggesting that FA grains are homozygous frameshift mutants.

OsIPK1 frameshift mutations disrupt Pi homeostasis and affect grain filling

To further investigate the effects of increased Pi content on FA formation, the grains of *0/+1(g4)* and *0/+1(g7)* were observed during grain filling (15 days after pollination). Two types of developing grains were identified. One was creamy white and gelatinous, and similar to WT, accounting for approximately three-quarters (81/110 for *0/+1(g4)*, 75/99 for *0/+1(g7)*), name it *plump(g4)* and *plump(g7)*, respectively. Another was a colorless liquid, which accounts for about a quarter, and is named *FA(g4)* and *FA(g7)* (Fig. 6A). Paraffin sections revealed that the *plump* grains were similar to WT, and had an endosperm rich in starch granules and a normally developed embryo, whereas *FA* grains only had an intact seed coat, however an aborted embryo and no starch granules (Fig. 6A).

To identify the genotypes of FA grains in these mutants, we isolated the embryo, seed coat, and colorless endosperm and performed a sequencing separately.

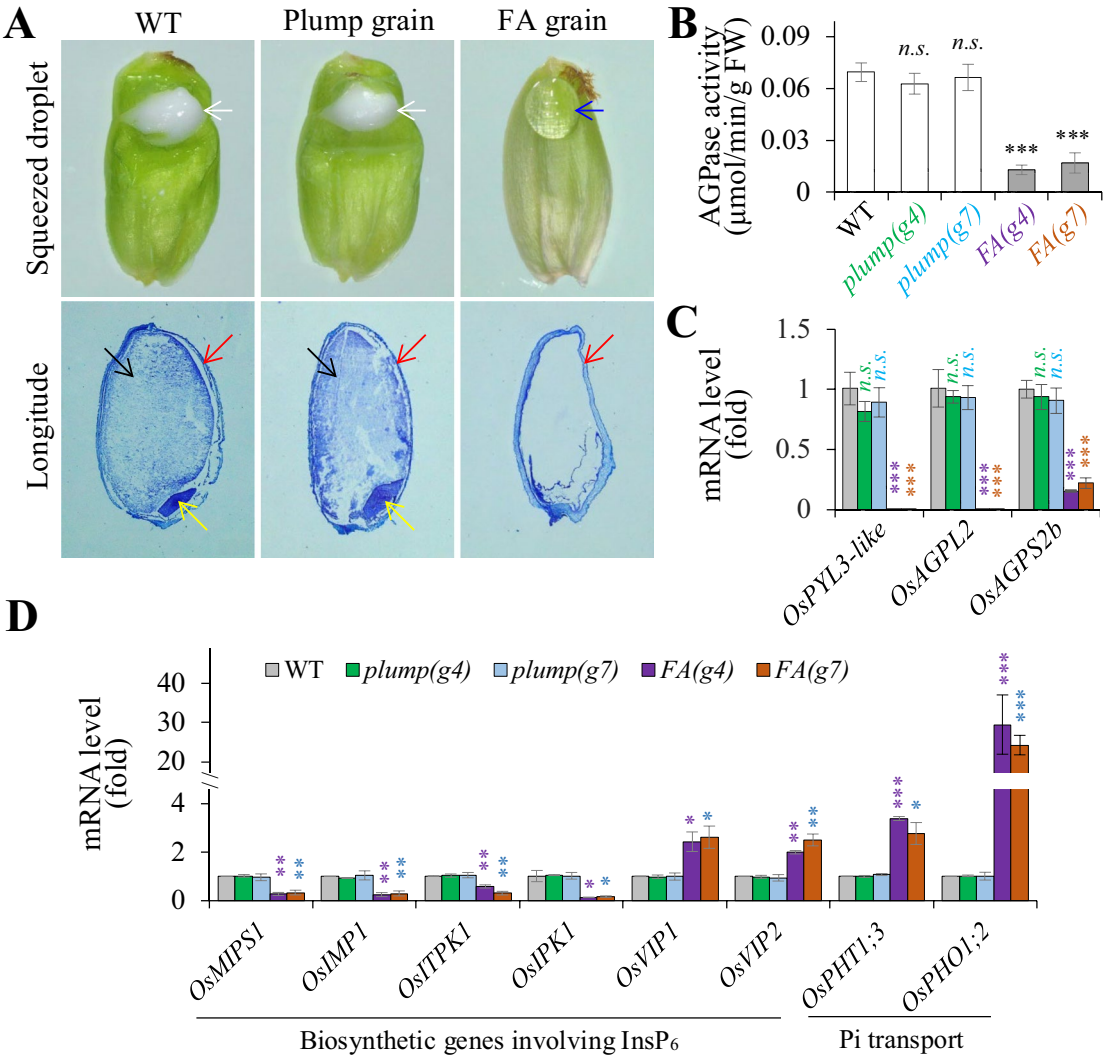

Fig. 6 *OsIPK1* frameshift mutations result in excessive Pi accumulation and impaired starch synthesis, and then produces FA grain during the filling stage. **A** The morphology and the longitudinal section stained with 0.1% toluidine blue of developing grains (15 days after fertilization). The white arrows represent developed endosperm, while the blue arrows represent undeveloped endosperm, and the black, red, and yellow arrows represent the stained longitudinal section of endosperm, seed coat, and embryo, respectively. **B** AGPase activity in the plump grains and the corresponding FA grains during the grain-filling stage. Data are shown as means ± SE (μmol/min/g FW). **C** Expression of *OsPYL3-like*, *OsAGPL2*, and *OsAGPS2b* and **D** genes involved in inositol phosphate metabolism and Pi transport in cells. Data are shown as means ± SE (fold) ($N = 3$ biological repeats; $n = 3$ technical repeats). Student's *t*-tests: *, $P < 0.05$, **, $P < 0.01$; ***, $P < 0.001$, *ns* no significant difference

Unfortunately, we could not identify normal peak (homozygous genotype) in these tissues (Table S5). In contrast, we could identify normal and overlapping peaks in the plump grains (Table S5), indicating that the embryos of FA grain were aborted, which was due to homozygous lethality, as only the embryo represents the genotypes of the offspring.

To investigate the biochemical mechanism of abnormal filling in FA grain, $InsP_6$, Pi, and carbohydrate content of FA grain during the filling stage were analyzed. Compared with WT, *FA (g4* and *g7)* exhibited a reduction in $InsP_6$ content by 27.7–29.6%, an increase in Pi content by 2.24–2.34-fold, a decrease in starch content by 11.9–14.0%, and an increase in sucrose content by 2.52–2.85-fold, while soluble sugar content showed no difference (Fig. S6), which was consistent with those of mature grains.

To further investigate the relationship between $InsP_6$ and Pi with starch levels in the *FA (g4* and *g7)* grain filling, the activity of a key enzyme involved in starch synthesis (AGPase) was studied. AGPase activity in *FA(g4* and *g7)* was only 18.5 to 24.2% of that in the WT, while that in the *plump(g4* and *g7)* was not different from that in the WT (Fig. 6B).

OsPYL3-like (*Os06g0528300*) is uniquely expressed in the endosperm and its expression pattern is closely related to grain filling in rice (Zhou 2015). *OsAGPL2* and *OsAGPS2b* encode the large and small AGPase subunits, respectively (Lee et al. 2007). The expression of *OsPYL3-like* and *OsAGPL2* was nearly abolished in *FA(g4* and *g7)* (0.2–1.0% and 0.1–0.7% of the WT, respectively), whereas the expression of *OsAGPS2b* was only 15.6–22.1% of the WT. In contrast, their expression in plump seeds was similar to that in the WT seeds (Fig. 6C). These results suggested that the frameshift mutations result in impaired starchy endosperm synthesis and grain filling are terminated in FA grains.

Moreover, the expression of genes upstream (*OsMIPS*, *OsIMP*, *OsITPK1*, and *OsIPK1*) of the $InsP_6$ synthesis was reduced by 13.6–58.0% of the WT, whereas the expression of genes (*OsVIP1* and *OsVIP2*) involved in inositol pyrophosphate synthesis, downstream of the $InsP_6$ synthesis, was increased (2.0–2.61-fold of the WT) in *FA(g4* and *g7)*. Furthermore, the expression of genes related to Pi transport (*OsPHT1;3*) and Pi efflux (*OsPHO1;2*) was increased (2.8–3.4-fold and 24.2–29.4-fold of the WT, respectively) in *FA(g4* and *g7)* (Fig. 6D). Whereas in plump grains (*g4* and *g7*), the expression of these genes did not differ from that of the WT. Taken together, these data suggest that *OsIPK1* frameshift mutations disturb IP metabolism and Pi homeostasis, and impair the starchy endosperm synthesis, which in turn produces FA grains.

Discussion

Seeds are not only food for humans, but also the reproductive organs of crops. However, the accumulation of high levels of $InsP_6$ in grains causes human health problems and environmental pollution. Breeding low $InsP_6$ crops is an important global issue. It is not known whether IPK1, the enzyme that catalyzes the final step in $InsP_6$ synthesis, is a promising target for breeding *lpa* crops. In this study, *OsIPK1* in rice was knocked out by CRISPR/Cas9 technology and demonstrated that *OsIPK1* frameshift mutations result in excessive Pi accumulation, decreased starch synthesis during grain filling, and consequently decreasing grain yield in rice. Therefore, *lpa* breeding should be performed cautiously when selecting *OsIPK1* as a target in rice.

OsIPK1 is an essential gene in rice, and its disruption results in homozygous lethality

Essential genes are critical cellular components, and their loss usually causes lethality (Lloyd et al. 2015). Among the genes that produce distinct phenotypes when lost, "essential" genes that produce lethal phenotypes have always been the target of research as they possess functions essential for the survival of organisms and are potential drug targets in microorganisms. In plants, essential genes are often single-copy genes, widely expressed, slowly evolving, and highly connected in functional gene networks (Lloyd et al. 2015).

In this study, all the gRNAs in the coding sequence (*CDS*) were unable to obtain homozygous frameshift mutants (Table 1), indicating that frameshift mutations result in homozygous lethality. However, the expression of *OsIPK1* under its native promoter in biallelic frameshift mutants could obtain homozygous frameshift plump seeds in transgenic lines (Fig. S2B). Our results were consistent with those of Jiang et al. (2021), who were unable to obtain homozygous mutants with one- and two-base deletions in the third exon of *OsIPK1*. Furthermore, only one copy of *OsIPK1* (*Os04g56580*), which is a characteristic essential gene, has been identified in the rice genome (Suzuki et al. 2007). Therefore, *OsIPK1* is proposed as an essential gene in rice, and its disruption results in homozygous lethality.

The reduced seed-setting rate in *OsIPK1* frameshift mutants was due to abnormal grain development

Seed-setting rate is a major component that determines grain yield. Several factors result in a reduced seed-setting rate. These include defective pollen grains, abnormal double fertilization, and defective embryonic and endosperm development (Xu et al. 2017). In this study, yield traits,

especially seed-setting rate, were observed to be significantly decreased in biallelic and heterozygous frameshift mutants (Fig. 2). The reduced seed-setting rate in *OsIPK1-indel* frameshift plants contrasts with the observations in the following reports, such as those *IPK1* mutants generated using RNAi technique in rice (Ali et al. 2013) or wheat (Aggarwal et al. 2018), or by CRISPR/Cas9 in wheat (Ibrahim et al. 2022) and soybean (Song et al. 2022). This inconsistency may be because RNAi only downregulates *IPK1* expression and does not completely disrupt the function of proteins. Another possibility is that the disruption of *IPK1* could be compensated by homologous genes, as three (Bhati et al. 2014; Ibrahim et al. 2022) or two (Yuan et al. 2007) homologous genes were identified in wheat and soybean, respectively, whereas *OsIPK1* is a single-copy gene in rice (Suzuki et al. 2007).

To investigate factors resulting in reduced seed-setting rate determined by homozygous lethality revealed that although floret morphology was normal (Fig. 3A), pollen viability was significantly decreased in the biallelic or heterozygous mutants (Fig. 3B, C). Increased accumulation of Pi in the anthers was reported to decrease pollen vitality in mutants of the phosphorus transporter regulatory gene *OsNLA1* (Yang et al. 2020). Therefore, the reduction in pollen viability in *OsIPK1-indel* may be attributed to an accumulation of Pi in the anthers. Further studies are required to substantiate this hypothesis. However, reciprocal-crossing experiments revealed that lowered pollen viability is not the fundamental reason for homozygous frameshift lethality (Table 2). Furthermore, a class of FA grains with normal seed coats, and no starchy endosperms, occurred in the mature grains of heterozygous mutants (Fig. 4A), whose frequency (21.92% in *0/+1(g4)*) almost reached the theoretical ratio of Mendelian recessive homozygotes (Fig. 4B). Therefore, we propose that the reduced seed-setting rate was due to abnormal grain development in frameshift mutants.

Blockage of $InsP_6$ synthesis disturbs Pi homeostasis and severely impairs starch synthesis during grain filling

In cereal seeds, endosperms store starch and proteins in the grains, and are the most important source of human food and animal feed. Cereal endosperm development progresses through coenocytic nuclear division, cellularization, aleurone, starchy endosperm differentiation, and the accumulation of storage products (Liu et al. 2022). Although genes affecting endosperm development have been reported, understanding of the accumulation of storage substances remains unclear.

In contrast to plump grains, $InsP_6$ synthesis was nearly completely blocked, whereas Pi content was significantly increased in *FA(g4* and *g7)* grains (Fig. 5), resulting in

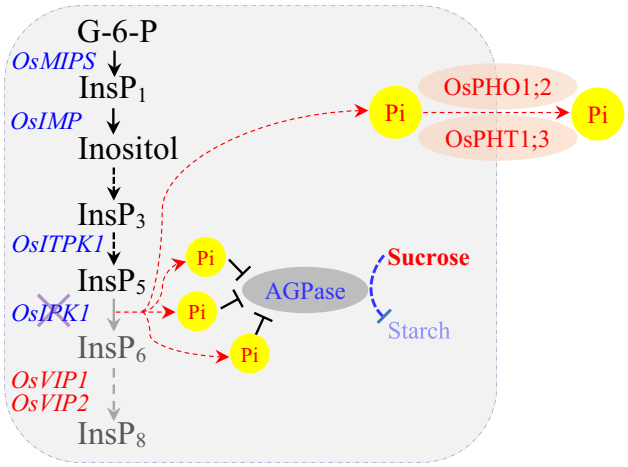

Fig. 7 A proposed model of grain-filling abortion in *OsIPK1* frameshift mutants. *OsIPK1* frameshift mutations result in a notably increased Pi content accompanied by a decrease in $InsP_6$ levels. The upstream genes responsible for $InsP_6$ synthesis are downregulated whereas the downstream genes of $InsP_6$ synthesis are upregulated. Simultaneously, excessive Pi inhibits AGPase activity, results in grain filling failure and further development into FA grains, and promotes the expression of *PHO1;2* and *PHT1;3* to transport the excessive Pi in FA grains. Blue: decreased; Red: increased

almost no starch synthesis in FA grains (Fig. 6A). This corresponded well with the increase in sucrose content, decrease in AGPase activity, and the expression of the specific transcripts *OsAGPL2* and *OsAGPS2b* was nearly abolished in seeds (Figs. 6B, C, S6). Moreover, the starch content in *OsIPK1-indel* plump grains decreased with increasing Pi content (Fig. S4), and the expression of the endosperm development marker gene *OsPYL3-like* was nearly abolished in *FA(g4* and *g7)* grains (Fig. 6C). Therefore, nearly complete blockage of $InsP_6$ synthesis significantly increases Pi content, inhibits starchy endosperm development, and produces FA grains. Further research is needed to determine whether abnormal endosperm development leads to the inhibition of starch synthesis or whether the two occur simultaneously. Our results were consistent with a mutation in the Pi efflux gene *OsPHO1;2*, which causes excessive Pi and inhibition of AGPase activity, ultimately resulting in developmental defects in the rice endosperm (Ma et al. 2021). A similar conclusion was also reported that much lower AGPase and starch phosphorylase activities in grains during filling stage is the main reason decreasing grain weight, low grain starch accumulation and poor plumpness in *os-lpa1*, a low $InsP_6$ mutant which was developed from Xieqingzao using ^{60}Co γ-ray (Zhao et al. 2008).

Moreover, the expression of upstream genes in $InsP_6$ synthesis was downregulated, whereas the expression of downstream genes was upregulated in *FA(g4* and *g7)* (Fig. 6D), with a clear pre- and post-phytate boundary, suggesting cascade regulation in $InsP_6$ synthesis. The expression of

OsPHO1;2 and *OsPHT1;3* was also upregulated in *FA* (Fig. 6D), suggesting that high levels of Pi are urgently required for efflux and phosphorus homeostasis has been destroyed in FA grains. Therefore, IPK1-mediated $InsP_6$ synthesis plays an important role in regulating grain phosphorus homeostasis, which is consistent with studies in *Arabidopsis* (Kuo et al. 2018; Gulabani et al. 2022).

In conclusion, the data in this study indicates that the *OsIPK1* frameshift mutations result in a notably increased Pi content accompanied by a decrease in $InsP_6$ levels during the filling stage. Then the activity of AGPase, which converts sucrose to starch, is inhibited, resulting in grain filling failure and further development into FA grains (Fig. 7). These results provide insights into the function and mechanism of OsIPK1 in maintaining phosphate homeostasis and grain filling in rice.

Supplementary Information The online version contains supplementary material available at https://doi.org/10.1007/s11103-024-01488-z.

Author contributions XC and DC conceived the research plan, supervised the experiments, analysed the data, and wrote and revised the paper. LW performed the experiments, collected and analysed the data, and wrote the original draft. JC, NZ, XW, JS and WY participated in experiments. MPV and SW revised the paper. All authors participated in the research and approved the final manuscript.

Funding This work was supported by grants from the Natural Science Foundation of Tianjin (No. 21JCYBJC00010), the Fundamental Research Funds for the Central Universities, Nankai University (No. 60), the National Natural Science Foundation of China (No. 32070349), and the creative group project of the Rice Industry Technological System of Tianjin (No. ITTRRS20211000-02).

Data availability Data will be made available on request.

Declarations

Conflict of interest The authors declare no conflicts of interest.

References

Aggarwal S, Kumar A, Bhati KK, Kaur G, Shukla V, Tiwari S, Pandey AK (2018) RNAi-mediated downregulation of inositol pentakisphosphate kinase (*IPK1*) in wheat grains decreases phytic acid levels and increases Fe and Zn accumulation. Front Plant Sci 9:259. https://doi.org/10.3389/fpls.2018.00259

Al Hasan SM, Hassan M, Saha S, Islam M, Billah M, Islam S (2016) Dietary phytate intake inhibits the bioavailability of iron and calcium in the diets of pregnant women in rural Bangladesh: a cross-sectional study. BMC Nutrit 2:24. https://doi.org/10.1186/S40795-016-0064-8

Ali N, Paul S, Gayen D, Sarkar SN, Datta K, Datta SK (2013) Development of low phytate rice by RNAi mediated seed-specific silencing of inositol 1,3,4,5,6-pentakisphosphate 2-kinase gene (*IPK1*). PLoS ONE 8:e68161. https://doi.org/10.1371/journal.pone.0068161

Bhati KK, Aggarwal S, Sharma S, Mantri S, Singh SP, Bhalla S, Kaur J, Tiwari S, Roy JK, Tuli R, Pandey AK (2014) Differential expression of structural genes for the late phase of phytic acid biosynthesis in developing seeds of wheat (*Triticum aestivum* L.). Plant Sci 224:74–85. https://doi.org/10.1016/j.plantsci.2014.04.009

Bohn L, Meyer AS, Rasmussen SK (2008) Phytate: impact on environment and human nutrition. A challenge for molecular breeding. J Zhejiang Univ-SC B 9:165–191. https://doi.org/10.1631/jzus.B0710640

Cominelli E, Pilu R, Sparvoli F (2020) Phytic acid and transporters: what can we learn from l*ow phytic acid* mutants? Plants 9:69. https://doi.org/10.3390/plants9010069

Cridland C, Gillaspy G (2020) Inositol pyrophosphate pathways and mechanisms: what can we learn from plants? Molecules 25:2789. https://doi.org/10.3390/molecules25122789

Doyle J (1991) DNA protocols for plants. In: Hewitt GM, Johnston AWB, Young JPW (eds) Molecular techniques in taxonomy. Springer, Berlin, pp 283–293

Fitzgerald MA, McCouch SR, Hall RD (2009) Not just a grain of rice: the quest for quality. Trends Plant Sci 14:133–139. https://doi.org/10.1016/j.tplants.2008.12.004

Freed C, Adepoju O, Gillaspy G (2020) Can inositol pyrophosphates inform strategies for developing low phytate crops? Plants 9:115. https://doi.org/10.3390/plants9010115

Gulabani H, Goswami K, Walia Y, Roy A, Noor JJ, Ingole KD, Kasera M, Laha D, Giehl RFH, Schaaf G, Bhattacharjee S (2022) *Arabidopsis* inositol polyphosphate kinases IPK1 and ITPK1 modulate crosstalk between SA-dependent immunity and phosphate-starvation responses. Plant Cell Rep 41:347–363. https://doi.org/10.1007/s00299-021-02812-3

Huang B, Hennen-Bierwagen TA, Myers AM (2014) Functions of multiple genes encoding ADP-glucose pyrophosphorylase subunits in maize endosperm, embryo, and leaf. Plant Physiol 164:596–611. https://doi.org/10.1104/pp.113.231605

Ibrahim S, Saleem B, Rehman N, Zafar SA, Naeem MK, Khan MR (2022) CRISPR/Cas9 mediated disruption of *Inositol Pentakisphosphate 2-Kinase 1* (*TaIPK1*) reduces phytic acid and improves iron and zinc accumulation in wheat grains. J Adv Res 37:33–41. https://doi.org/10.1016/j.jare.2021.07.006

Jeon JS, Ryoo N, Hahn TR, Walia H, Nakamura Y (2010) Starch biosynthesis in cereal endosperm. Plant Physiol Bioch 48:383–392. https://doi.org/10.1016/j.plaphy.2010.03.006

Jiang M, Liu Y, Li R, Li S, Tan Y, Huang J, Shu Q (2021) An inositol 1,3,4,5,6-pentakisphosphate 2-kinase 1 mutant with a 33-nt deletion showed enhanced tolerance to salt and drought stress in rice. Plants 10:23. https://doi.org/10.3390/plants10010023

Kim SI, Tai TH (2011) Identification of genes necessary for wild-type levels of seed phytic acid in *Arabidopsis thaliana* using a reverse genetics approach. Mol Genet Genomics 286:119–133. https://doi.org/10.1007/s00438-011-0631-2

Kuo HF, Chang TY, Chiang SF, Wang WD, Yy C, Chiou TJ (2014) *Arabidopsis* inositol pentakisphosphate 2-kinase, AtIPK1, is required for growth and modulates phosphate homeostasis at the transcriptional level. Plant J 80:503–515. https://doi.org/10.1111/tpj.12650

Kuo HF, Hsu YY, Lin WC, Chen KY, Munnik T, Brearley CA, Chiou TJ (2018) *Arabidopsis* inositol phosphate kinases IPK1 and ITPK1 constitute a metabolic pathway in maintaining phosphate homeostasis. Plant J 95:613–630. https://doi.org/10.1111/tpj.13974

Lee SK, Hwang SK, Han M, Eom JS, Kang HG, Han Y, Choi SB, Cho MH, Bhoo SH, An G, Hahn TR, Okita TW, Jeon JS (2007) Identification of the ADP-glucose pyrophosphorylase isoforms essential for starch synthesis in the leaf and seed endosperm of rice (*Oryza sativa* L.). Plant Mol Biol 65:531–546. https://doi.org/10.1007/s11103-007-9153-z

Li WX, Zhao HJ, Pang WQ, Cui HR, Poirier Y, Shu QY (2014) Seed-specific silencing of *OsMRP5* reduces seed phytic acid and weight in rice. Transgenic Res 23:585–599. https://doi.org/10.1007/s11248-014-9792-1

Li Q, Wang L, Zheng Y, Sun Y, Chen X, Chen D (2019) Editing rice phytate synthetase *IPK1* gene using CRISPR/Cas9 technology. Acta Sci Nat Univ Nankaiensis 52:52–59

Liu QL, Xu XH, Ren XL, Fu HW, Wu DX, Shu QY (2007) Generation and characterization of low phytic acid germplasm in rice (*Oryza sativa* L.). Theor Appl Genet 114:803–814. https://doi.org/10.1007/s00122-006-0478-9

Liu JX, Wu MW, Liu CM (2022) Cereal endosperms: development and storage product accumulations. Annu Rev Plant Biol 73:255–291. https://doi.org/10.1146/annurev-arplant-070221-024405

Lloyd JP, Seddon AE, Moghe GD, Simenc MC, Shiua SH (2015) Characteristics of plant essential genes allow for within- and between-species prediction of lethal mutant phenotypes. Plant Cell 27:2133–2147. https://doi.org/10.1105/tpc.15.00051

Ma B, Zhang L, Gao Q, Wang J, Li X, Wang H, Liu Y, Lin H, Liu J, Wang X, Li Q, Deng Y, Tang W, Luan S, He Z (2021) A plasma membrane transporter coordinates phosphate reallocation and grain filling in cereals. Nat Genet 53:906–915. https://doi.org/10.1038/s41588-021-00855-6

Murphy J, Riley JP (1962) A modified single solution method for the determination of phosphate in natural water. Anal Chim Acta 27:31–36. https://doi.org/10.1016/s0003-2670(00)88444-5

Pfister B, Zeeman SC (2016) Formation of starch in plant cells. Cell Mol Life Sci 73:2781–2807. https://doi.org/10.1007/s00018-016-2250-x

Poon JSY, Le Fevre RE, Carr JP, Hanke DE, Murphy AM (2020) Inositol hexakisphosphate biosynthesis underpins PAMP-triggered immunity to *Pseudomonas syringae* pv. *tomato* in *Arabidopsis thaliana* but is dispensable for establishment of systemic acquired resistance. Mol Plant Pathol 21:376–387. https://doi.org/10.1111/mpp.12902

Preiss J (1982) Regulation of the biosynthesis and degradation of starch. Annu Rev Plant Physiol 33:431–454. https://doi.org/10.1146/annurev.pp.33.060182.002243

Raboy V (1997a) Accumulation and storage of phosphate and minerals. In: Larkins BA, Vasil IK (eds) Cellular and molecular biology of plant seed development. Kluwer Academic Publishers, pp 441–477

Raboy V (2000) Low-phytic-acid grains. Food Nutrit Bull 21:423–427. https://doi.org/10.1177/156482650002100416

Raboy V (2001) Seeds for a better future: 'low phytate' grains help to overcome malnutrition and reduce pollution. Trends Plant Sci 6:458–462. https://doi.org/10.1016/s1360-1385(01)02104-5

Raboy V (1997b) Low phytic acid mutants and selection thereof. United States Patent PAT:US6111168

Sahu A, Verma R, Gupta U, Kashyap S, Sanyal I (2024) An overview of targeted genome editing strategies for reducing the biosynthesis of phytic acid: an anti-nutrient in crop plants. Mol Biotechnol 66:11–25. https://doi.org/10.1007/s12033-023-00722-1

Saiardi A, Erdjument-Bromage H, Snowman AM, Tempst P, Snyder SH (1999) Synthesis of diphosphoinositol pentakisphosphate by a newly identified family of higher inositol polyphosphate kinases. Curr Biol 9:1323–1326. https://doi.org/10.1016/s0960-9822(00)80055-x

Saripalli G, Gupta PK (2015) AGPase: its role in crop productivity with emphasis on heat tolerance in cereals. Theor Appl Genet 128:1893–1916. https://doi.org/10.1007/s00122-015-2565-2

Sharpley AN, Chapra SC, Wedepohl R, Sims JT, Daniel TC, Reddy KR (1994) Managing agricultural phosphorus for protection of surface waters: issues and options. J Environ Qual 23:437–451. https://doi.org/10.2134/jeq1994.00472425002300030006x

Shi J, Wang H, Hazebroek J, Ertl DS, Harp T (2005) The maize low-phytic acid 3 encodes a myo-inositol kinase that plays a role in phytic acid biosynthesis in developing seeds. Plant J 42:708–719. https://doi.org/10.1111/j.1365-313X.2005.02412.x

Silva VM, Putti FF, White PJ, Reis ARd (2021) Phytic acid accumulation in plants: biosynthesis pathway regulation and role in human diet. Plant Physiol Biochem 164:132–146. https://doi.org/10.1016/j.plaphy.2021.04.035

Song JH, Shin G, Kim HJ, Lee SB, Moon JY, Jeong JC, Choi H-K, Kim IA, Song HJ, Kim CY, Chung YS (2022) Mutation of *GmIPK1* gene using CRISPR/Cas9 reduced phytic acid content in soybean seeds. Int J Mol Sci 23:10583. https://doi.org/10.3390/ijms231810583

Stevenson-Paulik J, Odom AR, York JD (2002) Molecular and biochemical characterization of two plant inositol polyphosphate 6-/3-/5-kinases. J Biol Chem 277:42711–42718. https://doi.org/10.1074/jbc.M209112200

Stevenson-Paulik J, Bastidas RJ, Chiou ST, Frye RA, York JD (2005) Generation of phytate-free seeds in *Arabidopsis* through disruption of inositol polyphosphate kinases. Proc Natl Acad Sci USA 102:12612–12617. https://doi.org/10.1073/pnas.0504172102

Sun YY, Xu WZ, Wu L, Wang RZ, He ZY, Ma M (2016) An *Arabidopsis* mutant of inositol pentakisphosphate 2-kinase *AtIPK1* displays reduced arsenate tolerance. Plant Cell Environ 39:416–426. https://doi.org/10.1111/pce.12623

Suzuki M, Tanaka K, Kuwano M, Yoshida KT (2007) Expression pattern of inositol phosphate-related enzymes in rice (*Oryza sativa* L.): implications for the phytic acid biosynthetic pathway. Gene 405:55–64. https://doi.org/10.1016/j.gene.2007.09.006

Verbsky JW, Wilson MP, Kisseleva MV, Majerus PW, Wente SR (2002) The synthesis of inositol hexakisphosphate: characterization of human inositol 1,3,4,5,6-pentakisphosphate 2-kinase. J Biol Chem 277:31857–31862. https://doi.org/10.1074/jbc.M205682200

Wang X, Zhou W, Lu Z, Ouyang Y, Su OC, Yao J (2015) A lipid transfer protein, OsLTPL36, is essential for seed development and seed quality in rice. Plant Sci 239:200–208. https://doi.org/10.1016/j.plantsci.2015.07.016

Wang W, Xie Y, Liu L, King GJ, White P, Ding G, Wang S, Cai H, Wang C, Xu F, Shi L (2022) Genetic control of seed phytate accumulation and the development of low-phytate crops: a review and perspective. J Agric Food Chem 70:3375–3390. https://doi.org/10.1021/acs.jafc.1c06831

Wilson MP, Majerus PW (1997) Characterization of a cDNA encoding *Arabidopsis thaliana* inositol 1,3,4-trisphosphate 5/6-kinase. Biochem Bioph Res Co 232:678–681. https://doi.org/10.1006/bbrc.1997.6355

Xu Y, Yang J, Wang YH, Wang JC, Wan JM (2017) OsCNGC13 promotes seed-setting rate by facilitating pollen tube growth in stylar tissues. PLoS Genet 1:e1006906. https://doi.org/10.1371/journal.pgen.1006906

Yang X, Shears SB (2000) Multitasking in signal transduction by a promiscuous human Ins(3,4,5,6)P_4 1-kinase/Ins(1,3,4)P_3 5/6-kinase. Biochem J 351:551–555. https://doi.org/10.1042/BJ3510551

Yang SY, Lu WC, Ko SS, Sun CM, Hung JC, Chiou TJ (2020) Upstream open reading frame and phosphate-regulated expression of rice *OsNLA1* controls phosphate transport and reproduction1. Plant Physiol 182:393–407. https://doi.org/10.1104/pp.19.01101

Yuan FJ, Zhao HJ, Ren XL, Zhu SL, Fu XJ, Shu QY (2007) Generation and characterization of two novel low phytate mutations in soybean (*Glycine max* L. Merr.). Theor Appl Genet 115:945–957. https://doi.org/10.1007/s00122-007-0621-2

Yuan FJ, Zhu DH, Tan YY, Dong DK, Fu XJ, Zhu SL, Li BQ, Shu QY (2012) Identification and characterization of the soybean IPK1 ortholog of a low phytic acid mutant reveals an exon-excluding splice-site mutation. Theor Appl Genet 125:1413–1423. https://doi.org/10.1007/s00122-012-1922-7

Zhao NC, Zhang QF, Wu DX, Wei KS, Zhang XM, Cheng FM (2008) Characteristics of grain starch synthesis at filling stage and translocation of carbohydrates in leaves and sheaths for low phytic acid mutant rice. Acta Agron Sin 34:1977–1984. https://doi.org/10.1016/S1875-2780(09)60017-1

Zhou Y (2015) Screening of rice genes with highly endosperm-specificexpression pattern and preliminary analysis of the promoter of *Latex-1* gene [Master, Fujian Agricultural and Forest University] (in Chinese with English abstract)